Dependence of degree of orientation of copper oxide nuclei on oxygen pressure during initial stages of copper oxidation

Langli Luo,[1] Yihong Kang,[2] Zhenyu Liu,[2] Judith C. Yang,[2] and Guangwen Zhou[1,*]

[1]*Department of Mechanical Engineering & Multidisciplinary Program in Materials Science and Engineering, State University of New York, Binghamton, New York 13902, USA*

[2]*Department of Mechanical Engineering and Materials Science, University of Pittsburgh, Pittsburgh, Pennsylvania, 15261, USA*

(Received 26 August 2010; published 11 April 2011)

We report *in situ* transmission electron microscopy observations of the dependence of the degree of orientations of oxide nuclei on oxygen pressure during the initial-stage oxidation of Cu(100) surfaces, which reveal a transition from nucleating epitaxial Cu_2O islands to randomly oriented oxide islands with increasing the oxygen pressure from 5×10^{-5} to 150 Torr. We show by a kinetic model that this transition of oxide nucleation orientation is driven by the influence of oxygen pressure on the oxide nucleation barrier and atom collision rate.

DOI: 10.1103/PhysRevB.83.155418 PACS number(s): 81.16.Pr, 68.55.A−, 82.40.−g

I. INTRODUCTION

The oxidation of metals plays a key role in many technological and environmental processes such as corrosion, chemical catalysis, fuel reactions, and thin-film processing. Over the past decades, surface science studies on the oxidation of metal surfaces under idealized conditions, i.e., ultrahigh vacuum (UHV), have gathered a wealth of knowledge including the surface structure, adsorption sites, and reaction pathways. However, the resulting profound understanding of the reaction mechanism obtained under rarefied UHV conditions does not automatically translate into an equally good understanding of the technologically relevant realistic (or near-) atmospheric oxidation. It has been shown recently that the surface oxidation proceeds readily under high-pressure oxidation conditions, but appears not to proceed under the low-pressure conditions typical of a vacuum experiment, despite favorable thermodynamics. For example, using a combination of *in situ* surface x-ray diffraction, scanning tunneling microscopy, and density-functional-theory calculations, Lundgren *et al.* have studied the oxidation of Pd surfaces from UHV to atmospheric pressure and found that the formation of PdO bulk oxides requires a surprising significantly larger oxygen pressure than that predicted by first-principles atomistic thermodynamics.[1–4] Similar behavior has been observed during the initial oxidation of other metals such as Rh (Refs. 5 and 6) and Cu.[7–10] Therefore, it is highly desirable to bridge this pressure gap by determining the difference in the response of a metal surface exposed to both the low and high pressures of oxygen gas.

Herein, we present a very demonstrative example of how the difference in oxygen pressure can lead to different behaviors of oxide nucleation during the initial oxidation of Cu surfaces. It has been shown previously that the oxidation of copper and many other metals proceeds via nucleation of oxide islands,[11–16] which are assumed to have thermodynamically controlled orientations.[17] Here we show that this is the case only if the metal surface is oxidized under a relatively low oxygen pressure (pO_2), and that increasing the oxygen pressure will lead to nucleation of randomly oriented islands. Our kinetic model reveals that this nucleation orientation transition is driven by the opposite effect of oxygen pressure on two critical factors governing the nucleation of oxide islands, i.e., the nucleation barrier and atom collision rate.

II. EXPERIMENT

Our experiments were carried out in a modified JEOL 200CX transmission electron microscope (TEM).[18] This microscope is equipped with UHV chamber with base pressure $\sim 10^{-8}$ Torr. The microscope was operated at 100 KeV to minimize the possibility of radiation effects on oxidation behavior. A leak valve attached to the column permits the controlled introduction of oxygen gas directly into the microscope at a pO_2 between 5×10^{-5} and 760 Torr. Cu(100) films with ~600-Å thickness were grown on NaCl(100) substrates by *e*-beam evaporation. The metal films were removed from the substrate by flotation in deionized water, washed, and mounted on a TEM sample holder that allows for resistive heating to a maximum temperature of 1000 °C. Any native Cu oxide is removed by annealing the films in the TEM under vacuum conditions at ~750 °C (Ref. 19) or by *in situ* annealing in methanol vapor at a pressure of 5×10^{-5} Torr but lower temperature (~350 °C), resulting in a clean copper surface.[20]

III. EXPERIMENTAL RESULTS

After admitting oxygen gas into the TEM chamber, no oxide islands appear on the clean Cu surfaces within the first couple of minutes. Visible oxide islands are then observed to nucleate rapidly and reach their saturation number density after several minutes of oxidation time. The saturation time depends on the oxygen pressure, i.e., the higher the oxygen pressure, the faster the oxidation rate for reaching the saturation of nucleation. For instance, the saturation time is ~10 min for the oxidation under $pO_2 = 5 \times 10^{-3}$ Torr, while it is ~2 min under $pO_2 =$ 150 Torr. Further oxidation leads to the growth and coalescence of oxide islands. Figure 2 shows the dependence of the saturated number density of the oxide islands as a function of the oxygen pressure from 5×10^{-4} to 150 Torr. It can be seen that, increasing the oxygen pressure from $pO_2 = 5 \times 10^{-4}$ to $pO_2 = 150$ Torr increases the saturation density of oxide islands by four orders of magnitude. The observation

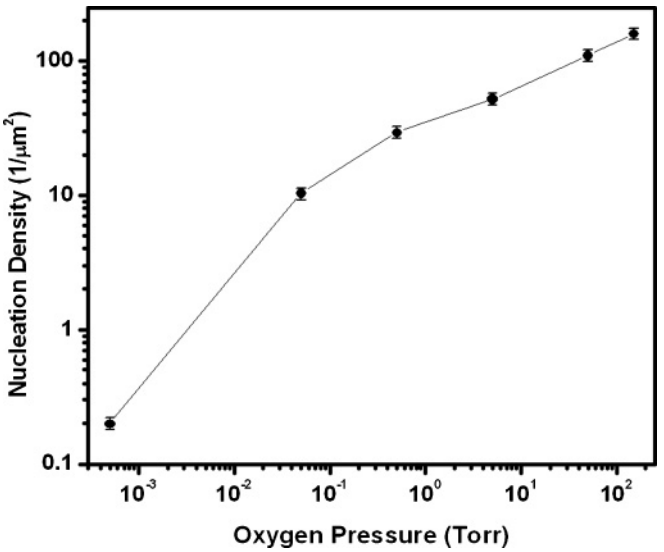

FIG. 1. The dependence of the saturation number density of oxide islands as a function of oxygen pressure is measured using *in situ* TEM imaging of the oxidation of Cu(100) surfaces at 350 °C and oxygen pressure ranging from 5×10^{-4} to 150 Torr.

that the density of oxide nuclei saturates suggests that the nucleation process is limited by oxygen surface diffusion, i.e., an active zone of oxygen capture exists around each oxide island. The radius of this oxygen capture zone is proportional to the collision rate of oxygen atoms by oxygen surface diffusion and free-energy barrier of forming an oxide nucleus. The higher density of oxide islands correlates with a smaller zone of oxygen capture, which implies that increasing the oxygen pressure leads to a faster oxygen collision rate and a smaller oxide nucleation barrier. It is rather surprising to note that the oxidation under $pO_2 = 150$ Torr still results in the nucleation of individual oxide islands rather than the continuous oxide film, despite the fast impingement rate of oxygen molecules onto the surface sites from the gas phase at this high oxygen pressure.

Figures 2(a)–2(c) show bright-field TEM images of Cu(100) surfaces oxidized at 350 °C and different pO_2 for 10 min. Oxide islands are observed to form on the surface and the density of oxide nuclei increases with increasing pO_2. Selected-area electron diffraction (SAED) patterns from the oxidized surfaces reveal that Cu_2O islands nucleated under the lower pO_2 (i.e., <5 Torr) have the cube-on-cube epitaxy with the Cu(100) substrate, i.e., (011)Cu_2O//(011)Cu and Cu_2O//Cu. Oxidation at $pO_2 = 150$ Torr and above results in the nucleation of nonepitaxial Cu_2O islands, as revealed by the presence of the Cu_2O diffraction ring pattern [Fig. 2(c)]. The intensity distribution over the diffraction rings is rather uniform, suggesting that the oxide islands are oriented at random. The appearance of additional diffraction spots or rings surrounding Cu reflections in the electron diffraction patterns shown in Fig. 2 is caused by the double diffraction of Cu and Cu_2O islands.

To check if any preferred orientations exist among the oxide islands formed under the high oxygen pressure, the ring

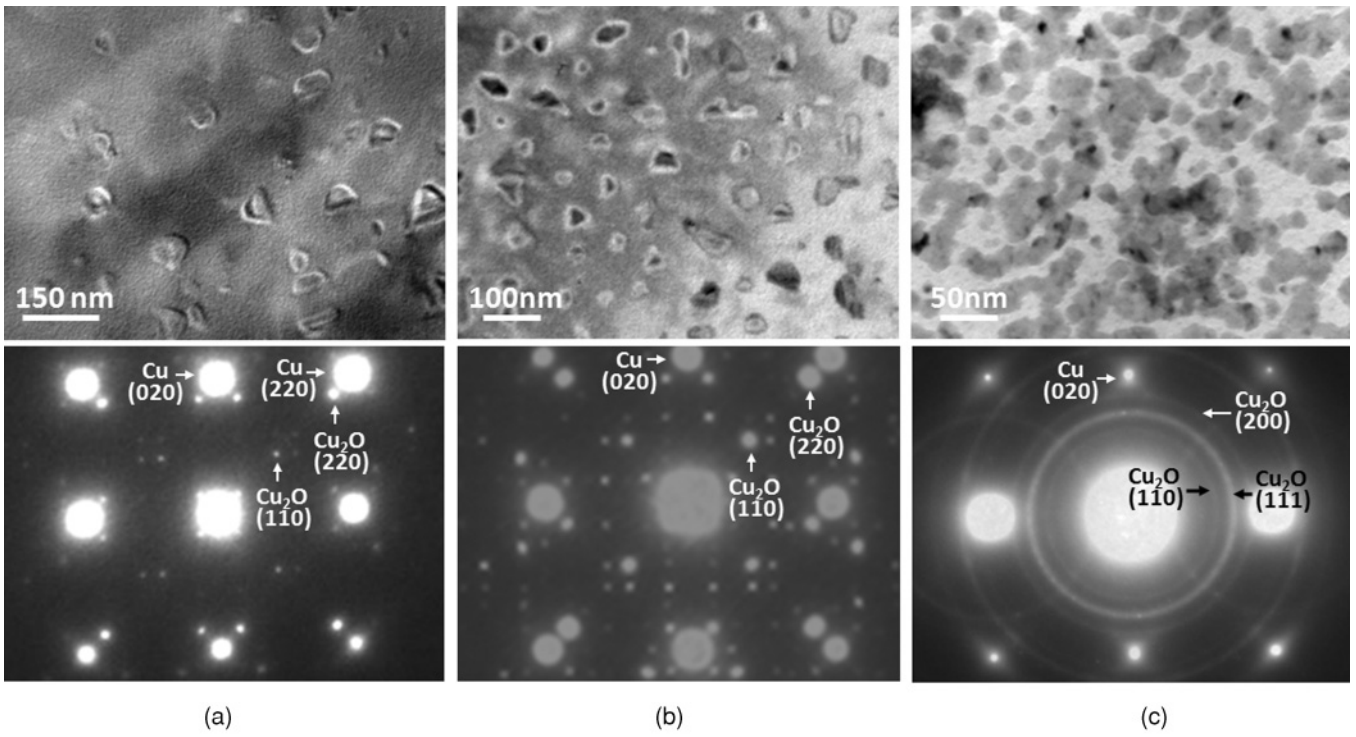

FIG. 2. Upper panel: Bright-field TEM images of Cu_2O islands formed Cu(100) oxidized at 350° C and different oxygen pressures for 10 min: (a) $pO_2 = 5 \times 10^{-4}$ Torr, (b) $pO_2 = 0.5$ Torr, and (c) $pO_2 = 150$ Torr. Lower panel: SAED patterns from the corresponding oxidized Cu(100) surfaces, where the additional reflections are due to double diffraction of electron beams by Cu and Cu_2O. A transition from nucleating epitaxial oxide islands to randomly oriented Cu_2O islands occurs upon increasing the oxygen pressure.

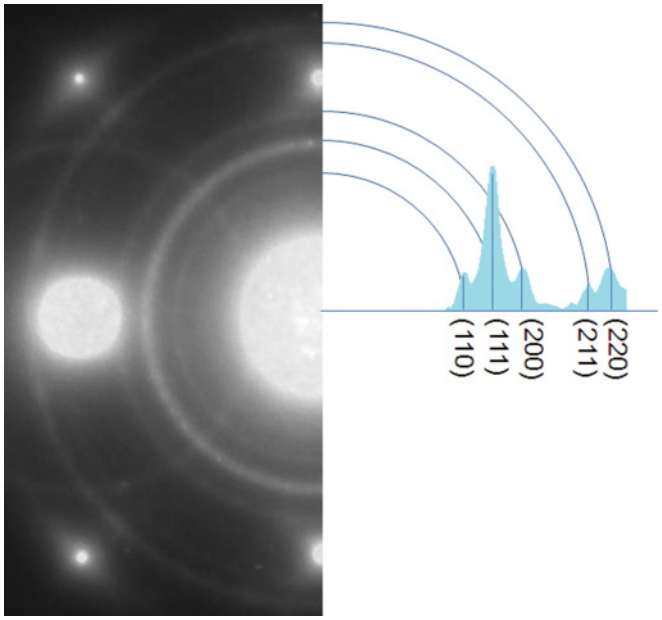

FIG. 3. (Color online) Intensity analysis and indexing of the electron diffraction ring pattern indicate that all rings allowed by the structure factors are present, suggesting the random orientations of Cu_2O islands formed on the Cu(100) surface.

diameters and integrated intensities of the electron diffraction pattern obtained from the oxidation at $pO_2 = 150$ Torr are measured by digital micrograph. Indexing of the ring pattern indicates that all rings allowed by the structure factors are present. The relative ring intensity along the radial direction is shown in Fig. 3. It can be seen that the intensity of the (111) ring is the strongest, the (200) ring is the second strongest, and the (211) ring has minimum intensity. Their relative intensity distribution matches qualitatively with the intensity ratios from x-ray Cu_2O powder diffraction [(110):(111):(200):(211):(220) = 9:100:37:1:27), suggesting the absence of preferred orientations (or texture structure) among the oxide islands formed under the high oxygen pressure.

Figure 4 shows the high-resolution (HR) TEM images of the oxidized Cu surfaces, which further confirm this pressure-dependent orientation of oxide nuclei. Figure 4(a) is a [001] zone-axis HRTEM image obtained from the Cu surface oxidized under $pO_2 = 0.5$ Torr, where the two-dimensional (2D) moiré fringe pattern caused by the overlapping of Cu_2O and Cu lattices is visible. The moiré fringes running parallel to {101} lattice planes of the Cu substrate suggest the Cu_2O islands have the cube-on-cube epitaxy with the Cu lattices, i.e., the equivalent planes and directions of Cu_2O islands and the Cu substrate are matched. Figure 4(b) is a [001] zone-axis HRTEM image of the Cu(100) surface oxidized under $pO_2 =$ 150 Torr, where the nonepitaxial nucleation of Cu_2O islands can be evidenced by the absence of strong 2D moiré fringe contrast and the inset Fourier transform pattern of the HRTEM image.

The above observations indicate that the oxidation under the high oxygen pressure results in the formation of randomly oriented oxide islands. However, an important question is whether the departure from the epitaxial orientation originates from the oxide island nucleation process or the later stages of oxide growth. As shown in Fig. 2, while the density of oxide islands increases with increasing oxygen pressure, the size distribution of the oxide islands formed under the different oxygen pressures is quite comparable for the same oxidation duration (i.e., $t = 10$ min). *Ex situ* atomic force microscopy (AFM) of the oxidized surfaces reveals that the island thickness is also similar for the different oxygen pressures. However, as it can be seen from Fig. 2(c), due to the larger island density for the oxidation at $pO_2 = 150$ Torr, some islands have begun to merge. Therefore, it is necessary to look at the effect of oxide growth and coalescence on the island orientations, particularly for the regime of the low oxygen pressures under which only epitaxial oxide islands are observed. Figure 5 shows bright-field TEM images and the corresponding electron

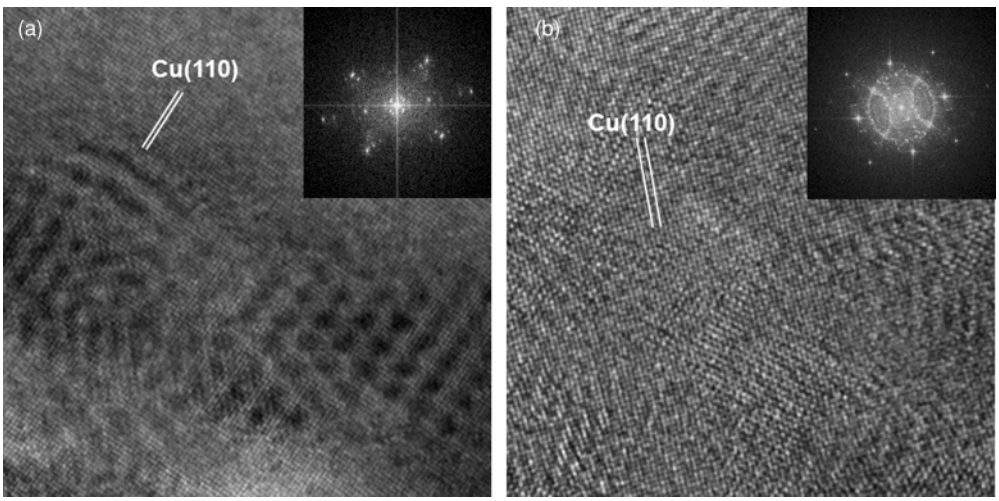

FIG. 4. HRTEM images of Cu(100) oxidized under different oxygen pressures. (a) $pO_2 = 0.5$ Torr and (b) $pO_2 = 150$ Torr. The strong 2D moiré fringe pattern implies the epitaxial nucleation of Cu_2O islands; the absence of 2D moiré fringes in (b) suggests the nonepitaxial nucleation of Cu_2O islands on the surface. The inset is the Fourier transform of the HRTEM images, which reveal the similar diffraction patterns as shown in Fig. 1.

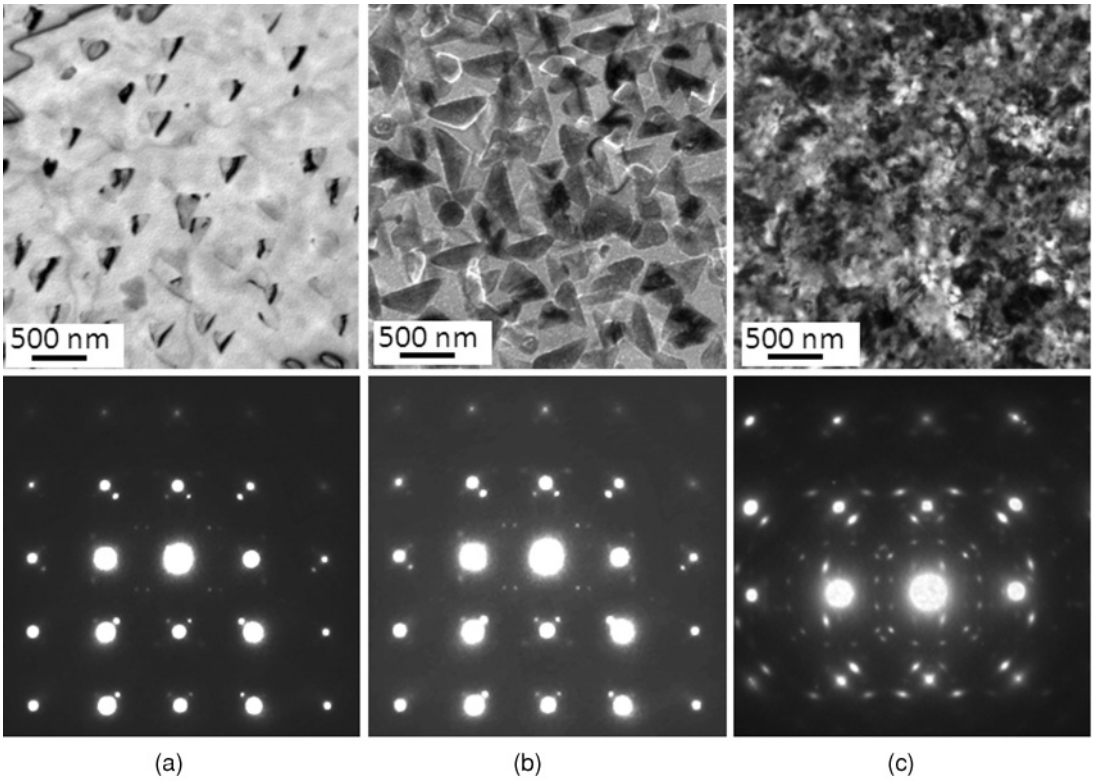

FIG. 5. Upper panel: Bright-field TEM images of Cu_2O islands formed Cu(100) oxidized at 350° C and different oxygen pressures for 30 min: (a) $pO_2 = 0.5$ Torr, (b) $pO_2 = 5$ Torr, and (c) $pO_2 = 50$ Torr. Lower panel: SAED patterns from the corresponding oxidized Cu(100) surfaces. The observations reveal that the cube-on-cube epitaxial orientation is still maintained during the growth and coalescence processes of the oxide islands.

diffraction patterns from the Cu surfaces oxidized at 350 °C for 30 min with $pO_2 = 0.05$, 5, and 50 Torr, respectively. Compared with the sizes of oxide islands as shown in Fig. 2, where the samples are oxidized for only 10 min, the longer oxidation time results in the increase in the island sizes. For the lower oxygen pressures ($pO_2 = 0.05$ and 5 Torr), individual islands are still visible on the Cu surfaces, while the oxidation under $pO_2 = 50$ Torr results in the coalesced and continuous oxide film. As can be seen from the corresponding electron diffraction patterns, the oxidized Cu surfaces with oxide islands or the coalesced oxide film still show the cube-on-cube epitaxial orientation of the oxide with the Cu substrate. By comparing with the diffraction patterns in Fig. 2, it can be noted that the oxide islands do not undergo significant changes in their crystallographic orientations during the growth and coalescence processes. These observations suggest that the orientation of an oxide island is largely determined at the very early stages of the oxide-island nucleation processes.

IV. DISCUSSION

To understand this pressure-dependent orientation of oxide nuclei, we first look at the effect of oxygen pressure on the nucleation barrier for the heterogeneous nucleation of an oxide island on a metal surface. During the nucleation process, an oxide nucleus increasing its size by growing should overcome an energy barrier for a given $\Delta\mu$ ($\Delta\mu$ is the chemical potential difference between the actual and equilibrium oxygen pressures during the oxidation) before it can become a stable island on the surface. Considering, for simplicity, the three-dimensional nucleation of an oxide island on a plane metal surface,[10,21,22] we can express the free energy of formation of a critical oxide embryo by

$$\Delta G^* = \frac{16\pi\sigma_{NO}^3}{3\Delta\mu^2} f(n), \tag{1}$$

where σ_{NO} denotes the specific interfacial energy between oxide nucleus and oxygen gas, θ is the contact angle of the oxide nucleus with the metal substrate, and $f(n) = \frac{(2+n)(1-n)^2}{4}$ is the geometrical factor for a plane surface. n depends on the interaction and structural match between the oxide nucleus and the metal substrate, and is related to the interfacial tension between the oxide and metal substrate by

$$n = (\sigma_{SO} - \sigma_{NS})/\sigma_{NO}, \tag{2}$$

where σ_{NS} and σ_{SO} are the interfacial free energies between the oxide nucleus and metal substrate and the substrate and oxygen gas, respectively. For a given system, the strong interaction and ideal structural match (i.e., epitaxial nucleation) leads to $n \to 1$; on the other hand, the weak interaction and poor structural match (i.e., nonepitaxial nucleation) leads to $n \to -1$.[23–26] These two situations are shown schematically in Fig. 6(a). Therefore, heterogeneous nucleation of oxide islands occurs in the range of between n = 1 and –1.

We then consider the oxide nucleation kinetics, which is defined as the number of stable nuclei created per area time. O_2

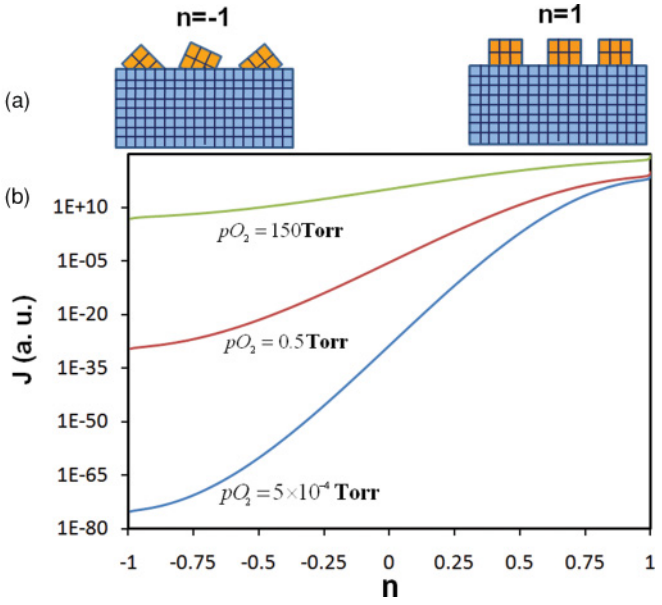

FIG. 6. (Color online) (a) Illustration of the relation between the structural match and the interfacial interaction parameter n: the strong interaction and good structural match leads to $n \rightarrow 1$, while weak interaction and poor structural match leads to $n \rightarrow -1$. (b) Plots of the relative steady-state nucleation rate J/B vs the interaction parameter n at different oxygen pressures pO_2 for the oxidation of Cu at 350 °C.

arriving from the vapor phase dissociates and migrates on the metal surface and then reacts with substrate atoms to produce oxide clusters of different sizes, thus giving rise to critical nuclei. In classic nucleation theory, the rate of forming critical nuclei results from a two-step process, i.e., the formation of a near equilibrium concentration N^* of critical nuclei and the impingement rate of adatoms w^* upon these critical nuclei. The nucleation rate J can thus be expressed as

$$J = \omega^* N^* \Gamma, \tag{3}$$

where N^* is density of critical nuclei, w^* is flux of attachment of adatoms to a critical nucleus, and Γ is the Zeldovich factor accounting for the deviation of the system from the equilibrium state.

The impingement of atoms onto a growing nucleus may occur by surface diffusion of adatoms to the nucleus periphery. The flux of oxygen towards the critical nucleus along the substrate surface can be calculated by

$$\omega^* = l^* D_s s \nabla (F\tau) \cong l^* D_s s \frac{F\tau}{a_0},$$

where I^* is the periphery of the critical nucleus on the substrate surface and is calculated as $\frac{4\pi\sigma_{NO}}{\Delta\mu}\sin\theta$, D_s is the oxygen atom jump rate, s is the oxygen sticking coefficient, F is the oxygen adsorption flux, τ is the oxygen residence time, and a_0 is the distance of a diffusion jump. D_s can be calculated by $D_s = a_0^2 v \exp(-\frac{E_{sd}}{kT})$, where a_0 is the distance of a diffusion jump, v is the vibration frequency of oxygen atoms, E_{sd} is the activation energy for O surface diffusion, k is the Boltzmann's constant, and T is the oxidation temperature. The oxygen adsorption flux F can be calculated from the kinetic gas theory and is equal to $\frac{pO_2}{\sqrt{2\pi mkT}}$, where pO_2 is the oxygen gas pressure and m is the molecular mass of oxygen. The residence time τ is equal to $\frac{1}{v}\exp(\frac{E_{des}}{kT})$, where E_{des} denotes the activation energy for desorption. Inserting l^* D_s, F, and τ into w^*, one obtains

$$\omega^* = \frac{4\pi a_0 s \sigma_{NO}}{\Delta\mu}\sin\theta\frac{pO_2}{\sqrt{2\pi mkT}}\exp\left(\frac{E_{des}-E_{sd}}{kT}\right). \tag{4}$$

The equilibrium density N^* of critical nuclei can be calculated from the nucleation barrier and the density of surface sites available for nucleation by $N^* = N_s \exp(\frac{-\Delta G^*}{kT})$, where ΔG^* is given in Eq. (1), N_s is the concentration of O atoms at the surface and is the product of the adsorption flux F, and the mean residence time τ, $N_s = \frac{p_{O_2}}{\sqrt{2\pi mkT}} \times \frac{1}{v_\perp}\exp(\frac{E_{des}}{kT})$. In order to account for the configurational entropy that arises from the number of ways of arranging islands on the sites, a statistical contribution $\Delta G_{conf} \approx -kT\ln(\frac{N_0}{N_s})$ is incorporated into the work of forming an oxide nucleus, where N_0 is the density of available oxygen adsorption sites. As a result, the density of critical oxide nuclei can be written as

$$N^* = N_s \exp\left(\frac{-\Delta G^* - kT\ln\left(\frac{N_0}{N_s}\right)}{kT}\right). \tag{5}$$

The Zeldovich factor Γ is to correct for the fact that some islands that have reached the critical size still decay to smaller sizes. For the formation of a cap-shaped nucleus at the given chemical potential $\Delta\mu$, Γ is given by[27]

$$\Gamma = \frac{\Delta\mu^2}{8\pi\Omega\sqrt{kT\sigma_{NO}^3 f(\theta)}}, \tag{6}$$

where Ω is the volume of oxygen atoms in the oxide phase. For the oxidation of Cu, $2Cu + \frac{1}{2}O_2 = Cu_2O$, the chemical potential $\Delta\mu$ can be written as $\Delta\mu = -\frac{1}{2N_A}RT\ln(\frac{pO_2}{pO_2^e})$, where N_A is the Avogadro constant, R is the gas constant, T is the oxidation temperature, pO_2 is the actual oxygen pressure during the oxidation, and pO_2^e is the equilibrium oxygen pressure as given by the Ellingham diagram for most metal oxides.[28] By substituting w^*, N^*, and Γ using the expressions of (1)–(6) into Eq. (3), the oxide nucleation rate J is obtained as

$$\frac{J}{B} = J_0 \exp\left(-\frac{16\pi\Omega^2(2+n)(1-n)^2}{3(kT)^3\left[\ln\left(\frac{pO_2}{pO_2^e}\right)\right]^2}\sigma_{NO}^3\right), \tag{7}$$

with

$$J_0 = \left[\frac{4(1+n)}{(2+n)(1-n)}\right]^{1/2}\left(\frac{pO_2}{pO_2^e}\right)\ln\left(\frac{pO_2}{pO_2^e}\right)$$

and

$$B = \frac{a_0 s N_0 pO_2^e}{4\sqrt{2\pi m\sigma_{NO}}}\exp\left(\frac{E_{des}-E_{sd}}{kT}\right),$$

where J_0 can be called the collisional prefactor.

Equation (7) indicates that the nucleation rate depends on both the oxygen pressure pO_2 and the metal-oxide structural match through the interaction parameter n. In Fig. 6(b), the nucleation rate J is plotted via n for different pO_2 for oxidation

of copper at 350 °C. As can be seen from the plots, the oxidation is dominated by nucleating epitaxial islands (i.e., $n = 1$) for the low oxygen pressure. With increasing pO_2, the nucleation rate of nonepitaxial oxide islands ($n \to 0$ and –1) is promoted and the difference in the nucleation rates of epitaxial and nonepitaxial oxide islands is significantly reduced. Therefore, both epitaxial and nonepitaxial Cu_2O islands are nucleated simultaneously on the metal surface under the high oxygen pressure. While the comparison between the experiment and the model can not be made quantitatively by Eq. (7) in terms of the island nucleation rate, due to the practical limitation of the classic heterogeneous nucleation theory (no accurate values for surface and interface energies as function of oxygen pressure, surface diffusion values, etc., makes the theory difficult to quantify), the real data of the experimental oxygen pressure are used in the model to predict the effect of oxygen pressure on the nucleation orientations of oxide islands. This effect can be noted in Fig. 6 and the outcome of the model provides a reasonable match with the ranges of the oxygen pressures at which epitaxial or nonepitaxial oxide islands are experimentally observed, as shown in Figs. 2–5, where the oxidation of Cu(100) under low pO_2 (<50 Torr) is dominated by nucleating epitaxial Cu_2O islands, while the oxidation under the higher pressure of $pO_2 = 150$ Torr results in randomly oriented Cu_2O islands. In addition, as shown in Fig. 1, the nucleation density of oxide islands for oxidation at $pO_2 = 10^{-4}$ and 150 Torr are comparable within four orders of magnitude, which agrees with the plots in Fig. 6, which show that J is comparable for both within a few orders of magnitude for 10^{-4} Torr to have $n = 1$, and 150 Torr to have n ranging from $n = -1$ to 1.

The above results indicate that the epitaxial nucleation of oxide islands can not be maintained within the whole range of oxygen pressures. The change in the nucleation orientation under different oxygen pressures can be physically understood as follows. At low oxygen pressure, the nucleation barrier is very high, i.e., the nucleation rate is dominated by the exponential term in Eq. (7). The top priority to accelerate the nucleation kinetics is to lower the nucleation barrier. Therefore, heterogeneous nucleation with the strong interaction and good structural match ($n \to 1$) between an oxide island and the metal substrate will be kinetically favored. Conversely, at high oxygen pressures, the nucleation barrier is reduced and the exponential term becomes less important. Instead, the issue of effective collisions, described by the collisional prefactor J_0 of Eq. (7), becomes important. The nucleation of oxide islands with weak interaction and poor structural match ($n \to 0$ and –1) with the metal substrate is enhanced. Kinetically speaking, to obtain the epitaxial oxide film on the metal substrate by oxidation, the oxygen pressure should be relatively low. If the oxygen pressure is too high, the kinetics leads to a deviation of nucleating oxide islands from the orientation of the metal substrate and the epitaxial relation will be lost.

V. CONCLUSION

In conclusion, the effect of oxygen pressure on the nucleation orientation of oxide islands during initial oxidation of metals is examined both experimentally and theoretically. The oxidation under the low oxygen pressures leads to epitaxial oxide islands, while increasing oxygen pressure results in randomly oriented oxide nuclei. It is shown that such a nucleation orientation transition is caused by the opposite effect (i.e., epitaxial versus nonepitaxial) of oxygen pressure on the nucleation barrier and atom collision rates. While nucleation takes place on the nanometer scale, its influence extends to larger size scale in controlling the microstructure evolution of the oxide film developed during metal oxidation. The insight obtained from this study is expected to have broader implications in understanding and manipulating the transient oxidation of metals under ambient working atmosphere as well as in the microstructure control of oxide films for many technological applications.

ACKNOWLEDGMENTS

This research was supported by the US Department of Energy, Office of Basic Energy Sciences, Division of Materials Sciences and Engineering, under Award No. DE-FG02-09ER46600.

*Author to whom correspondence should be addressed: gzhou@binghamton.edu

[1] E. Lundgren, J. Gustafson, A. Mikkelsen, J. N. Andersen, A. Stierle, H. Dosch, M. Todorova, J. Rogal, K. Reuter, and M. Scheffler, Phys. Rev. Lett. **92**, 046101 (2004).

[2] R. Westerstrom, C. J. Weststrate, J. Gustafson, A. Mikkelsen, J. Schnadt, J. N. Andersen, E. Lundgren, N. Seriani, F. Mittendorfer, G. Kresse, and A. Stierle, Phys. Rev. B **80**, 125431 (2009).

[3] R. Westerstrom, J. Gustafson, A. Resta, A. Mikkelsen, J. N. Andersen, E. Lundgren, N. Seriani, F. Mittendorfer, M. Schmid, J. Klikovits, P. Varga, M. D. Ackermann, J. W. M. Frenken, N. Kasper, and A. Stierle, Phys. Rev. B **76**, 155410 (2007).

[4] S. Ferrer, M. D. Ackermann, and E. Lundgren, MRS Bull. **32**, 1010 (2007).

[5] J. Gustafson, A. Mikkelsen, M. Borg, E. Lundgren, L. Kohler, G. Kresse, M. Schmid, P. Varga, J. Yuhara, X. Torrelles, C. Quiros, and J. N. Andersen, Phys. Rev. B **92**, 126102 (2004).

[6] J. Gustafson, A. Resta, A. Mikkelsen, R. Westerstrom, J. N. Andersen, E. Lundgren, J. Weissenrieder, M. Schmid, P. Varga, N. Kasper, X. Torrelles, S. Ferrer, F. Mittendorfer, and G. Kresse, Phys. Rev. B **74**, 035401 (2006).

[7] J. A. Eastman, P. H. Fuss, L. E. Rehn, P. M. Baldo, G. W. Zhou, D. D. Fong, and L. J. Thompson, Appl. Phys. Lett. **87**, 051914 (2005).

[8] K. Lahtonen, M. Hirsimaki, M. Lampimaki, and M. Valden, J. Chem. Phys. **129**, 124703 (2008).

[9] I. Lyubinetsky, S. Thevuthasan, D. E. McCready, and D. R. Baer, J. Appl. Phys. **94**, 7926 (2003).

[10] G. W. Zhou, Phys. Rev. B **81**, 195440 (2010).

[11]K. Heinemann, D. B. Rao, and D. L. Douglas, Oxid. Met. **11**, 321 (1975).
[12]P. H. Holloway and J. B. Hudson, Surf. Sci. **43**, 141 (1974).
[13]E. E. Hajcsar, P. R. Underhill, and W. W. Smeltzer, Langmuir **11**, 4862 (1995).
[14]G. W. Zhou and J. C. Yang, Phys. Rev. Lett. **89**, 106101 (2002).
[15]G. W. Zhou and J. C. Yang, Surf. Sci. **531**, 359 (2003).
[16]G. W. Zhou, D. D. Fong, L. Wang, P. H. Fuoss, P. M. Baldo, L. J. Thompson, and J. A. Eastman, Phys. Rev. B **80**, 134106 (2009).
[17]K. R. Lawless, Rep. Prog. Phys. **37**, 231 (1974).
[18]M. L. McDonald, J. M. Gibson, and F. C. Unterwald, Rev. Sci. Instrum. **60**, 700 (1989).
[19]G. W. Zhou and J. C. Yang, Phys. Rev. Lett. **93**, 226101 (2004).
[20]S. M. Francis, F. M. Leibsle, S. Haq, N. Xiang, and M. Bowker, Surf. Sci. **315**, 284 (1994).
[21]G. W. Zhou, Appl. Phys. Let. **94**, 201905 (2009).
[22]For mathematical simplicity, we neglect the effect of the nucleus embedment into the substrate. Our previous work shows that this nucleus embedment effect can cause approximately one order of magnitude difference in the critical oxygen pressure required for the nucleation of oxide islands (see Ref. 10).
[23]D. Turnbull and B. Vonnegut, Ind. Eng. Chem. **44**, 1292 (1952).
[24]X. Y. Liu, J. Chem. Phys **111**, 1628 (1999).
[25]X. Y. Liu, J. Chem. Phys **112**, 9949 (2000).
[26]X. Y. Liu, Langmuir **16**, 7337 (2000).
[27]I. V. Markov, *Crystal Growth for Beginners: Fundamentals of Nucleation, Crystal Growth, and Epitaxy* (World Scientific, Hackensack, 1995).
[28]D. R. Gaskell, *Introduction to Metallurgical Thermodynamics* (Scripta, Washington, DC, 1973).